

Patricio Lagos (plagos@astro.up.pt)

Instituto de Astrofísica e ciências do espaço - Centro de Astrofísica da Universidade do Porto, Portugal

## Goals and Sample:

Blue compact dwarf (BCD) galaxies, also known as HII galaxies, are low luminosity, low metallicity ( $7.0 < 12 + \log(O/H) < 8.4$ ) and gas-rich objects with optical spectra resembling those presented by HII regions. A small fraction of these galaxies fall in the regime of very low metallicity ( $12 + \log(O/H) < 7.6$ ) and are commonly refereed as extremely metal-poor (XMP) BCD galaxies. The morphologically diverse nature of BCD and XMP galaxies, allows us to consider the role played by galaxy interactions and the feedback between the star formation (SF) and the Interstellar medium (ISM) in the observed metal distributions. In this sense, these galaxies are the best nearby candidates for cosmologically young objects, as various arguments imply that they have formed most of their stellar mass in the past 1–3 Gyr (Papaderos et al 2008).

In this contribution, I review the results from our studies (Lagos et al. 2014, 2016) on the spatially resolved physical properties (abundances, kinematics, etc) of a selected sample of XMP star forming dwarf galaxies using GMOS (Gemini Program ID: GN-2010B-Q-69), and VIMOS (VLT Program ID: 090.B-0242) Integral Field Unit (IFU) spectroscopy. In those studies, we focus on the detection of metallicity gradients or inhomogeneities as expected if the ongoing star-formation activity is sustained by the infall or accretion of metal poor gas. The main properties of these galaxies are showed in Table 1.

Name	$M_B$ (mag)	D (Mpc)	$12 + \log(O/H)$	Scale (pc'')
HS2236+1344	-17.25	79.7	7.53	386
Tol 65	-15.44	38.5	7.55	184

Table 1. Main properties of our sample galaxies.

## Observations:

The VLT VIMOS-IFU observations were obtained using the gratings HR blue and orange covering a spectral range from  $\sim 3710$  to  $\sim 7700$  Å. Our data yield a scale on the sky of 0."33 per fiber. The Gemini GMOS-IFU observations were obtained using the grating R600 in one-slit mode with a projected diameter of 0."2 per fiber. In Figure 1 (left panels) we show Hubble Space Telescope (HST, filter F435W) and Gemini (g-band) images of the XMP BCD galaxies Tol 65 and HS2236+1344, respectively.

## Results:

### Gas Kinematics

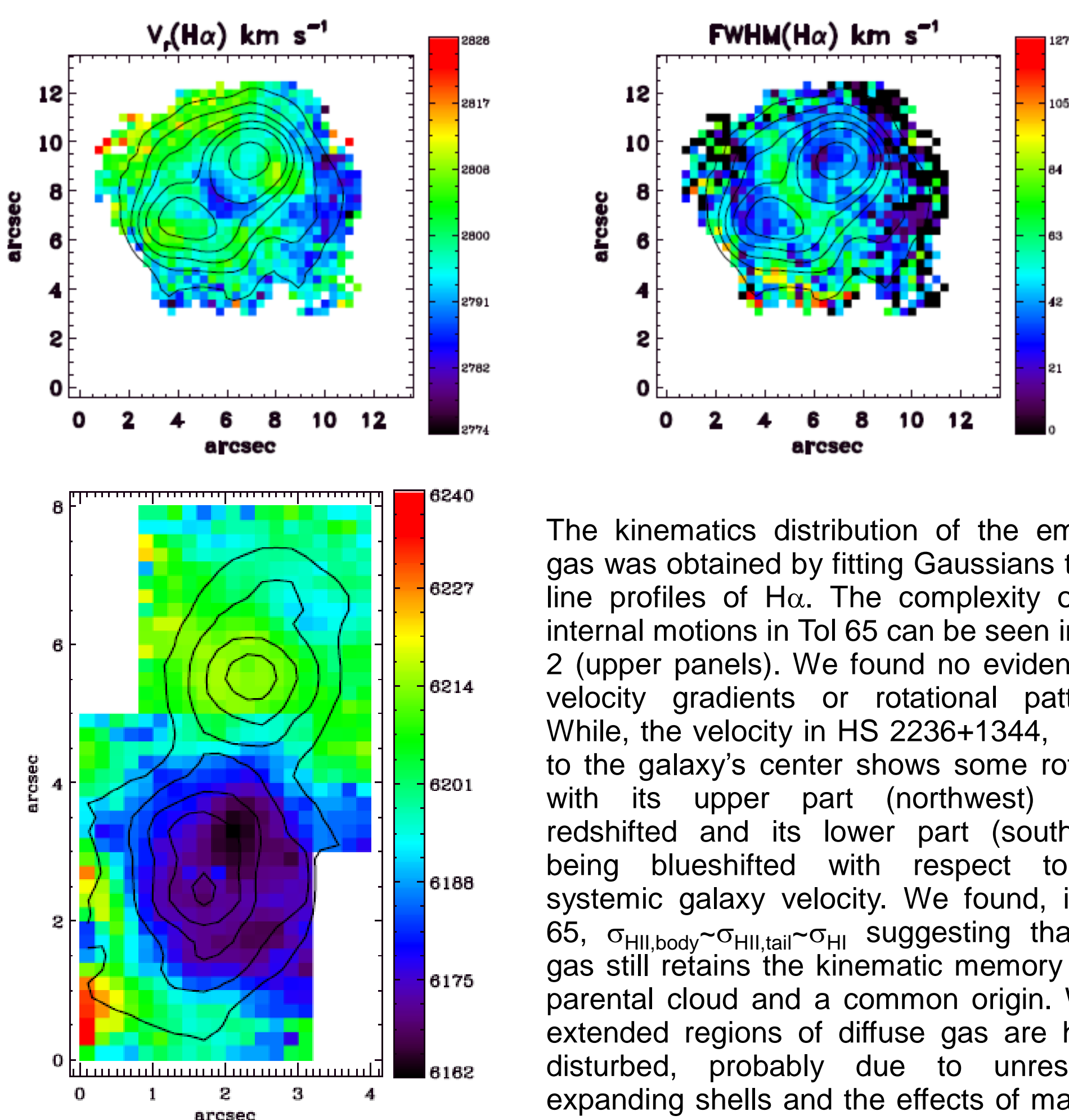


Figure 2.  $H\alpha$  radial velocity and FWHM of Tol 65 (upper panels) and  $H\alpha$  radial velocity of HS2236+1344 (lower panel). Contours display the  $H\alpha$  morphology.

The kinematics distribution of the emitting gas was obtained by fitting Gaussians to the line profiles of  $H\alpha$ . The complexity of the internal motions in Tol 65 can be seen in Fig. 2 (upper panels). We found no evidence of velocity gradients or rotational patterns. While, the velocity in HS 2236+1344, close to the galaxy's center shows some rotation with its upper part (northwest) being redshifted and its lower part (southeast) being blueshifted with respect to the systemic galaxy velocity. We found, in Tol 65,  $\sigma_{HII, body} \sim \sigma_{HII, tail} \sim \sigma_{HI}$  suggesting that the gas still retains the kinematic memory of its parental cloud and a common origin. While extended regions of diffuse gas are highly disturbed, probably due to unresolved expanding shells and the effects of massive star evolution. More details in Lagos et al. (2014, 2016).

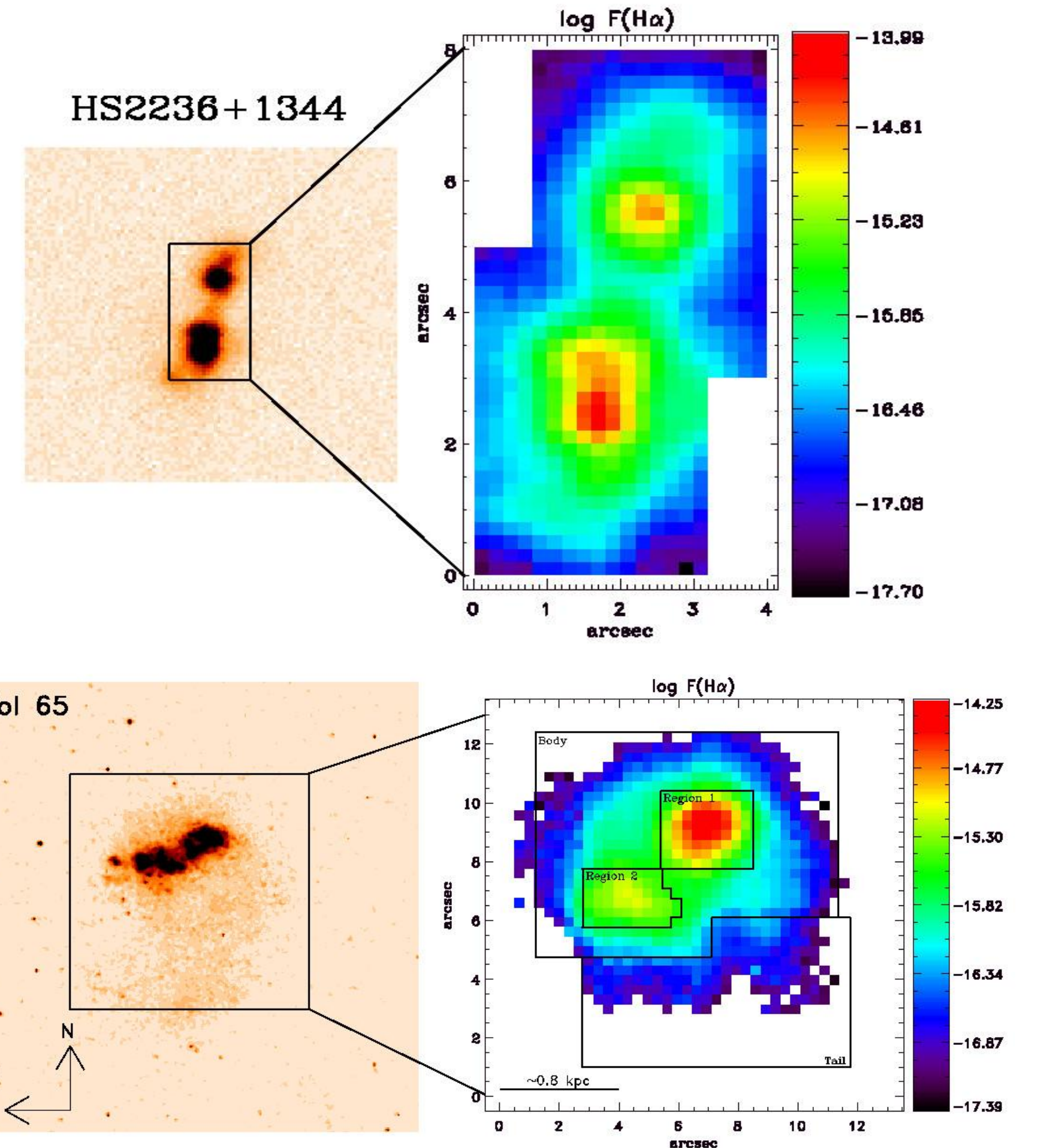


Figure 1. Left panels: Gemini g-band acquisition image and HST (filter F435W) images of the galaxies HS2236+1344 (Lagos et al. 2014) and Tol 65 (Lagos et al. 2016), respectively. Right panels:  $H\alpha$  emission line maps of the galaxies. Fluxes in units of  $\text{erg cm}^{-2} \text{s}^{-1}$ . The  $H\alpha$  maps show an extended morphology which reveal a clear nebular contribution in the outer part (underlying component) of the galaxies.

### Oxygen abundance

As far as the spatial distribution of oxygen abundances is concerned, we did not detect a statistically significant variation of metallicity along the galaxies. On the contrary, the oxygen and nitrogen appear to be well mixed across the ISM of these XMP galaxies (see Lagos & Papaderos 2013), suggesting a global and efficient transport and mixing by expanding starburst-driven super-shells (Lagos et al 2009 and references therein) and/or gas infall from the halo. For the sake of illustration, in Figure 3 we show the spatial distribution of  $12 + \log(O/H)$  in the galaxy Tol 65. We favour the idea that the most likely mechanisms to produce the flat abundance gradient and the cometary morphology in this XMP HII/BCD is the infall/accretion of cold gas from the outskirts of the galaxy or minor merger/interaction with an small companion recently in the past of the galaxy. This is in agreement with the scatter found between the gas metallicity ( $12 + \log(O/H)$ ) and SF rate at spaxel scales, Fig. 3 right panel, which clearly indicates that the metals in the ISM are almost fully diluted. More details in Lagos et al. (2016).

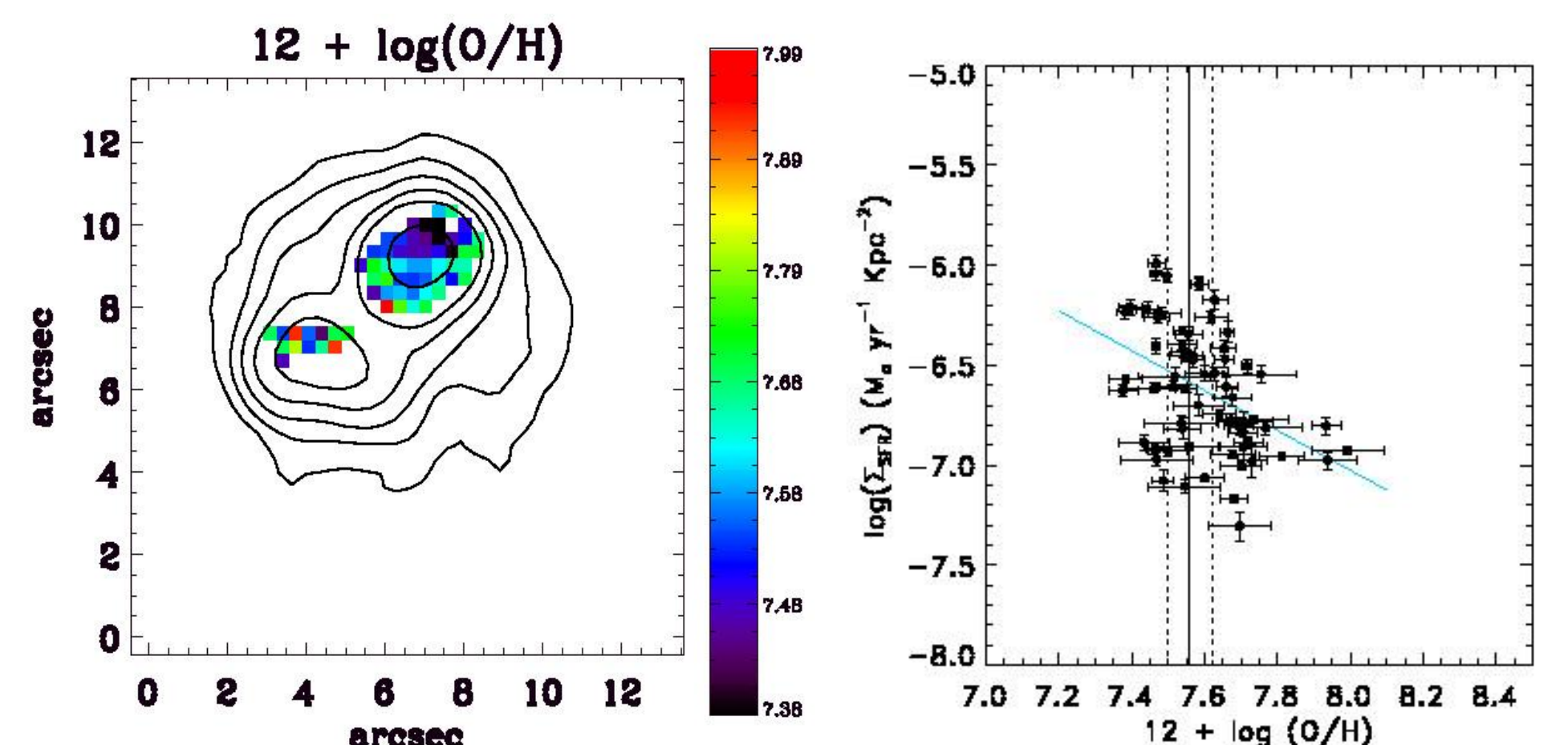


Figure 3. Left Panel:  $12 + \log(O/H)$  abundance map of Tol 65. Overlaid are the  $H\alpha$  flux contours. We considered spaxels with signal-to-noise ratio (S/N)  $> 3$  in the  $[OIII]\lambda 4363$  line. Right Panel: Relation between the SF rate surface density  $\Sigma_{sfr}$  and oxygen abundance  $12 + \log(O/H)$  at spaxel scales. The cyan line represents the linear fit to this relation. The  $12 + \log(O/H) = 7.56$  obtained in the main body of the galaxy is represented by the continuous line, while the errors at  $1\sigma$  level are in dotted lines.

## References:

- Lagos, P., Demarco, R., Papaderos, P., Telles, E., et al. 2016, MNRAS, 456, 1549
- Lagos, P., Papaderos, P., Gomes, J.M., et al. 2014, A&A, 569, 110
- Lagos, P., Papaderos, P. 2013, AdAst, 2013, 20
- Lagos, P., Telles, E., Muñoz-Tuñón, C., et al. 2009, AJ, 137, 5068
- Papaderos, P., Guseva, G., Izotov, Y. I., Fricke, K. J., 2008, A&A, 491, 113